Evaluation of Geological Hazard Susceptibility in Huixian City Based on AHP-IV

Maoqin Qin *

School of Civil Engineering, Henan Polytechnic University, Jiaozuo, China, 454003

* Corresponding Author Email: 15290469216@163.com

Abstract. This study presents a systematic evaluation of geohazard vulnerability in Huixian City, employing an informative model based on gully units integrated with hierarchical analysis (AHP-IV) to more accurately depict the geomorphic characteristics of geohazards. Utilizing ArcGIS and SPSS software, this study identified nine key evaluation indices: slope, Melton ratio, gully density, hazard point density, degree of undulation, rock group, normalized vegetation index (NDVI), soil erosion potential index (SPI), and multi-year average rainfall, facilitating a comprehensive assessment of geohazard vulnerability. Results showed that 36.13% of the study area was covered by zones with very high and high susceptibility., exhibiting concentrated geohazard development, while low susceptibility zones harbored fewer geohazard sites, consistent with actual distribution patterns. To validate the assessment results, this paper employed the frequency ratio model and ROC curve analysis. The frequency ratio demonstrated an increasing trend with escalating risk levels, with the very high susceptibility zone exhibiting significantly higher frequency ratios compared to the low susceptibility zone. Furthermore, the evaluation model achieved an AUC value of 0.871, indicative of its high precision and reliability, thus offering robust insights for geological hazard monitoring and early warning systems in Huixian City. This study not only enhances the practicality and guidance of geological hazard assessment but also furnishes a critical scientific foundation for geological hazard prevention and control efforts.

Keywords: Gully Unit, Informativeness Model, Analytic Hierarchy Process, Geological Hazards.

1. Introduction

Geological hazards present substantial challenges to urban development and safety worldwide. Conducting scientific evaluations of these hazards is essential for effective disaster prevention. This interdisciplinary field merges geology, engineering, and environmental science to tackle complex hazards and their determinants, constantly enhancing assessments to achieve greater accuracy and precision.

Currently, scholars worldwide focus on characterizing evaluation units, selecting indices, and developing models in geological hazard vulnerability assessment. Among these, evaluation models typically fall into two categories: single evaluation models, including the information quantity model [1], logistic regression model [2], and deterministic coefficient model [3], have been utilized for geohazard susceptibility assessment, exhibiting a certain degree of efficacy. Conversely, multivariate evaluation models have gained widespread traction among researchers due to their ability to comprehensively and accurately evaluate geohazard susceptibility. For example, Zhang et al. [4] used a combined deterministic coefficient and logistic regression model approach for assessing geological hazard susceptibility in Kaiyang County, Guizhou. Their results showed more accurate and logical zoning. Moreover, Cao et al. [5] evaluated geohazard susceptibility in the Song River Basin using the informativeness model and deterministic coefficient model, with results indicating the superiority of the informativeness model in assessing geohazard susceptibility within the study area.

These studies not only enhance the theoretical underpinnings and methodological approaches of geohazard susceptibility evaluation but also furnish critical scientific foundations for geohazard prevention and control endeavors.

This study uses the trench unit as the primary assessment unit for geological hazards due to its better spatial continuity, directional stability, and minimal boundary effects compared to traditional units like the grid or slope unit. Moreover, the single-information model presents certain drawbacks, including incomplete data and ambiguous parameters, which directly impact the accuracy of evaluation outcomes.To address these limitations, the Analytic Hierarchy Process (AHP)[6] method is employed. AHP, being a decision-making methodology grounded in hierarchical structuring, facilitates optimal decision-making by decomposing complex problems or decision factors to derive factor weights. In contrast to the single-information model, the AHP method can effectively mitigate its shortcomings, enhancing the overall accuracy and reliability of the evaluation process.

This study uses statistical analysis and integrates informativeness models with hierarchical analysis to evaluate geological hazard susceptibility at the ditch unit level in Huixian City, aiming to guide hazard prevention, control planning, and land management.

2. Overview of the study area

Huixian City, located in the western part of Xinxiang, Henan Province, China, spans 2007 km² and is situated where the Taihang Mountains meet the North China Plain [7]. It features a warm temperate continental monsoon climate and a terrain dominated by mountains and hills with a varied topography. The area has a dense river network, primarily formed by the Luo and Jian Rivers, and a complex geological structure that includes basement, sedimentary, and metamorphic rocks.

3. Data sources and evaluation modelling methods

3.1. Data sources

The primary data for this study encompass administrative boundary maps at a 1:1,000,000 scale, elevation imagery, geological hazard points, rainfall, vegetation cover (NDVI), and lithology data. These were sourced from various institutions, including the National Geographic Information Resource Catalog Service System, Geospatial Data Cloud, China Geological Survey Bureau, and the National Qinghai Tibet Plateau Scientific Data Center.

3.2. Division of evaluation units

This study used ArcGIS to detail the geomorphic features of a ditch network in Huixian City, located in southeast China. The network includes 421 ditches, spanning 754.2 km^2, and accounting for 51.2% of the city's area (Figure.1). Geographically, most ditches are found in the northwest's highlands, an area prone to large-scale geological disasters, in contrast to the southeast's plains, which feature low-lying terrain and dense vegetation. Consequently, there is a distinct spatial division in ditch density, with a higher concentration in the northwest and lower in the southeast.

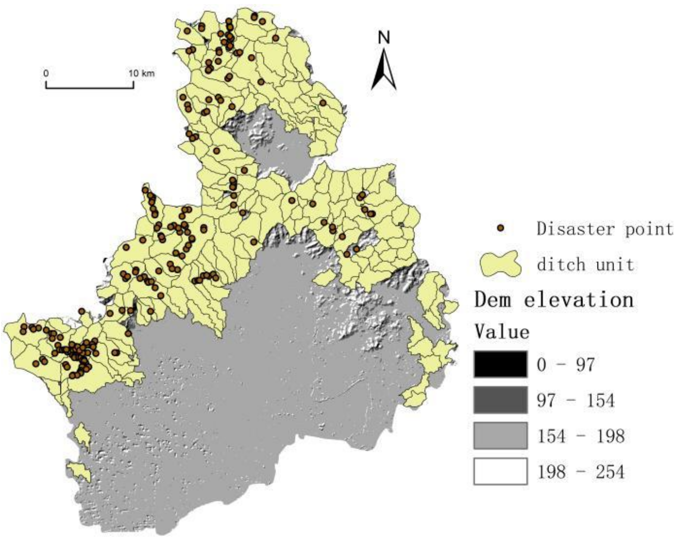

Figure 1. Division map of valley units in Huixian City

4. Evaluation model method

To more precisely determine the vulnerability of Huixian City, southeast China, to geological disasters, this study adopted a comprehensive method that integrates the Analytical Hierarchy Process (AHP) and the Information Volume Model (IV). AHP is a technique that breaks down complex issues into manageable hierarchical structures and factors. This process, relying on expert assessments and matrix development, calculates hierarchical rankings and ensures their consistency. This allows for the amalgamation of various layers to establish an overall ranking and evaluate its uniformity. Utilizing this technique, the study assigns specific weights to each evaluation criterion, reflecting their individual impact on geological disaster vulnerability.

The synergy of AHP and IV models facilitates a refined and detailed analysis of geological disaster risks in Huixian City, shedding light on the intricate web of factors that influence vulnerability. The Information Volume Model, in particular, underscores the complex interplay between geological disasters and their triggers by computing the information value of each influencing factor, thus quantifying their impact. Serving as a robust mechanism for gauging disaster susceptibility, this model employs principles of information theory to juxtapose the frequency of seismic occurrences triggered by particular factors against the general frequency of such events regionally. The methodology for quantifying the impact of specific factors on geological disasters is encapsulated in Formula (1).

$$I_{Aj \to B} = 10000 \times \ln \frac{N_j / N}{S_j / S} \tag{1}$$

In the Formula(1): $I_{Aj \to B}$ —The amount of information on the occurrence of geological disasters corresponding to the state (or interval) distribution of factors *A* and *j*. N_j —The number of geological hazard points corresponding to the state (or interval) distribution of factors *A* and *j*. *N*—The total number of disaster points with known geological hazard distribution in the research area. S_j —The area of the ditch unit where factors *A* and *j* are distributed in state (or interval). *S*—the total area of the ditch unit in the research area.

When the information quantity index exceeds zero, it indicates a high prevalence of geological disasters occurring under the prevailing conditions of factors A and j. Conversely, when the index value is negative, it suggests that the factors A and j are not conducive to the occurrence of geological disasters. When the index value is zero, it implies that the factors A and j do not provide any information about the occurrence of geological disasters, thereby necessitating their exclusion from the evaluation process.

$$I_{Aj \to B} = 10000 \times \sum_{i=1}^{n} \ln \frac{N_j / N}{S_j / S} \tag{2}$$

In the Formula(2): $I_{Aj \to B}$ —The amount of information on the occurrence of geological disasters corresponding to the state (or interval) distribution of factors *A* and *j*. N_j —The number of geological hazard points corresponding to the state (or interval) distribution of factors *A* and *j*. *N*—The total number of disaster points with known geological hazard distribution in the research area. S_j —The area of the ditch unit where factors A and j are distributed in state (or interval). *S*—the total area of the ditch unit in the research area. *n*—The total number of selected evaluation factors.

5. Grading of evaluation indicators

This study selected nine evaluation indicators for geological disaster susceptibility assessment: slope, Melton ratio, gully density, hazard point density, relief, rock group, normalized vegetation index (NDVI), soil erosion potential index (SPI), and annual average rainfall Furthermore, the paper refines grading standards for each indicator and examines how these factors, at all levels, relate to the frequency and extent of geological disasters.

5.1. Slope

Slope measures the surface's steepness, defined as the ratio of vertical height to horizontal distance. The paper categorizes slopes into five intervals for evaluation: 2~7, 7~11, 11~14, 14~18, and 18~34 degrees (Figure 2(a)). Among them, there are 182 disaster points with slopes between 18 and 34, accounting for 83.48% of the total. There are 8 disaster points with slopes between 2 and 7, accounting for 3.7% of the total. It can be seen that the density of geological hazard points gradually increases with the increase of slope. This trend is due to the northwest part of the study area being mountainous, with steep terrain and slopes, thus highly susceptible to geological disasters. Conversely, the southeast, being a plain with gentle terrain, is less prone to such disasters (Figure 3(a)).

5.2. Melton ratio

The Melton ratio indicates the basin's topography, with higher values signifying steeper terrain and lower values indicating gentler slopes. In geological disasters, mobilizing various materials requires significant energy. Given the terrain characteristics, the Melton ratio can reflect the potential energy for material movement within the basin, thereby influencing the ability to transport materials.

$$R_{\mathrm{M}} = \frac{\mathrm{d}H}{\sqrt{A}} \tag{3}$$

In the Formula(3): A—watershed area/m^2. dH—watershed height difference/m.

The Melton ratio in the Huixian City watershed is divided into five levels: 0.0015~0.0045, 0.0045~0.0075, 0.0075~0.01, 0.01~0.014, and 0.014~0.046 (Figure 2(b)). Statistical analysis indicates a clear trend: as the Melton ratio increases, so does the density of disaster points (Figure 3(b)). Notably, the highest concentration of geological hazards, at 51.02 points/100km^2, is found in areas with a Melton ratio ranging from 0.014 to 0.046. This suggests that the terrain within this range is markedly steeper and more prone to hazards.

5.3. Gully density

Gully density, defined as the total length of gullies per unit area, illustrates the degree of landscape erosion by water channels. It reflects the interaction of various factors, including topography, weather conditions, vegetation cover, land utilization, precipitation, runoff, and soil properties, among others.

In the Huixian City watershed, gully density is divided into five categories: <0.2, 0.2~0.35, 0.35~0.5, 0.5~0.6, and 0.6~2.2 (Figure 2(c)). Statistical analyses show a clear pattern: as gully density increases, so does the concentration of hazard points, peaking at 43.03 points/100km^2 for densities between 0.6 and 2.2. This trend highlights that areas with higher gully densities are more prone to significant land disintegration and decreased cohesion of surface materials, leading to enhanced surface water flow and intensified soil erosion (Figure 3(c)).

5.4. Disaster density

Disaster density, which quantifies the frequency or number of disaster events occurring in a particular area relative to its size, provides an insightful measure of the susceptibility of an area to geological disasters. It reflects the frequency and concentration of disasters within a specific region.

$$D = N / A \tag{4}$$

In the Formula (4) :D—Density of disaster points (number/m^2). N—the number of disaster points in a certain area.A—area area/m^2.

Within the Huixian City watershed, disaster point density is classified into five levels: <0.2, 0.2~0.4, 0.4~0.5, 0.5~0.7, and 0.7~2.8 (Figure 2(d)). There is a direct correlation between increased disaster point density and a heightened risk of geological disasters. This pattern is linked to several factors, including abundant material sources, adverse engineering geological conditions, and increased seismic activity in areas with high disaster point densities.

5.5. Roughness

Topographic relief, which quantifies the maximum relative elevation difference within a particular area, serves as a key indicator of landform characteristics. It is quantified through the Formula (5):

$$R = H_{\max} - H_{\min} \tag{5}$$

In the Formula (5): R—represents terrain relief. H_{max}—Represents the maximum elevation value within unit area. H_{min}—Represents the minimum elevation value within unit area.

The terrain relief within Huixian City's watershed is divided into five levels: 3~13, 13~18, 18~25, 25~35, and 35~67 (Figure 2(e)). Statistical analyses show a clear trend: as the degree of relief increases, so does the concentration of disaster points. Specifically, disaster point density peaks at 60.82 points/100 km^2 for relief degrees between 35 and 67. This correlation underscores the complex interplay between terrain relief and the processes of erosion, transportation, and deposition of surface materials. Consequently, areas with higher relief are more prone to instability of surface materials and an increased risk of geological disasters.

5.6. Engineering geological rock formations

Engineering geological rock groups [8] provide essential insights into the characteristics of the rock and soil within a specific area. The study categorizes the rock formations in Huixian City into four groups based on rock mass structure: soft rock, loose soil, hard rock, and interbedded soft and hard layers (Figure 2(f)). Interbedded soft and hard layers, which cover the largest area, are primarily found in the western region. The distributions of hard rock and loose soil are relatively similar, mainly located in the eastern region, reflecting the diversity in rock mass structures across different areas. Soft rocks, making up the smallest proportion, are concentrated in the northern region. Disaster points are mostly found within areas of interbedded soft and hard rock layers (Figure 3(f)), attributed to their prevalent unfavorable geological conditions.

5.7. Watershed vegetation coverage (NDVI)

Vegetation crucially influences the formation and stabilization of geological disasters [9]. Sparse vegetation increases river erosion and soil instability, with numerous exposed rocks and severe weathering creating a conducive environment for geological disasters. The Normalized Difference Vegetation Index (NDVI) in the study area is segmented into five levels: 0.43~0.67, 0.67~0.75, 0.75~0.78, 0.78~0.8, and 0.8~0.85 (Figure 2(g)). Generally, dense vegetation mitigates the risk of geological disasters, such as debris flows and landslides, by reducing rainwater infiltration into slopes. From Figure 3(g), disaster points are observed to cluster more in areas with higher NDVI values. While vegetation significantly affects the occurrence of geological disasters, factors like topography, soil conditions, and seismic activities also play critical roles and can lead to disasters regardless of vegetation coverage.

5.8. Basin average runoff erosivity index (SPI)

The Soil Erosion Potential Index (SPI)[10] gauges the erosive impact of surface runoff on the soil, with higher SPI values indicating stronger erosion. The SPI in the study area is divided into five levels: -3.8~-1.9, -1.9~-1.75, -1.75~-1.3, -1.3~-0.5, and -0.5~5.3 (Figure 2(h)). Statistical analysis shows an increase in disaster point density with rising SPI values, owing to the erosive action of regional water flows on surface soil, which heightens soil instability and the likelihood of geological disasters.

$$SPI = \ln\left(\frac{A_c}{L_c}\tan\beta\right) \tag{6}$$

In the Formula(6): A_c —catchment area upstream of the grid unit to be calculated/m^2. L_c —Grid unit width/m. $\tan\beta$ —The grid slope tangent value to be calculated.

5.9. Average rainfall in flood season for several years

Rainfall, a critical water source condition, significantly influences the occurrence of geological disasters. This study divides the average rainfall in Huixian City during the flood season (June to September) from 2020 to 2022 into five levels: <45mm, 45~150mm, 150~220mm, 220~350mm, and 350~535mm (Figure 2(i)). Statistical analyses demonstrate that disaster point density escalates with increasing rainfall, peaking at 48.72 points/100 km^2 (Figure 3(i)). This trend is linked to the profound impact of heavy rainfall on factors such as soil saturation, reduction in shear strength, and enhancement of surface runoff and erosion. Furthermore, rainfall is instrumental in generating surface runoff, which can significantly erode soil and alter the stress conditions of rock and soil, thereby elevating the risk of geological disasters.

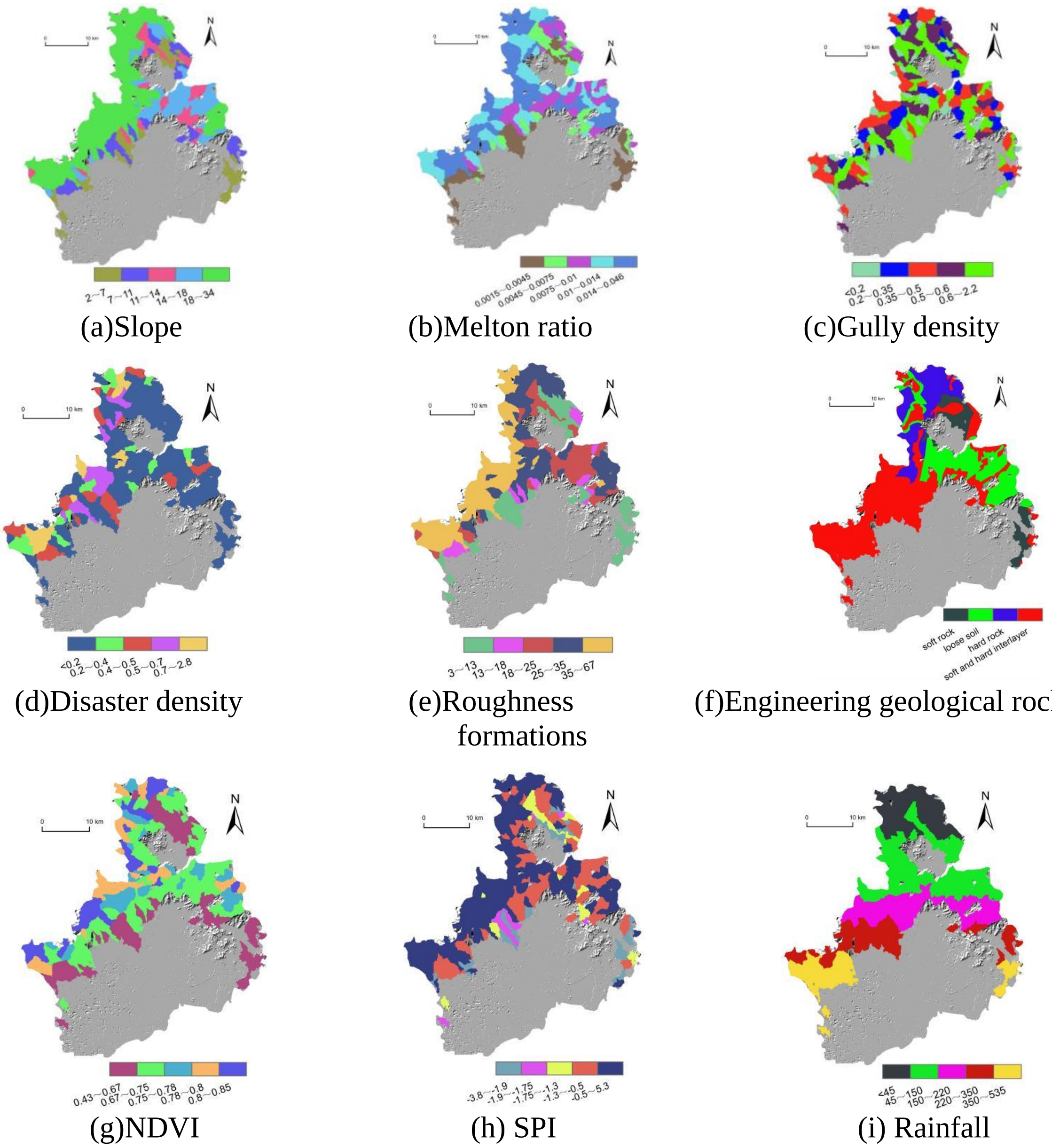

(a)Slope (b)Melton ratio (c)Gully density

(d)Disaster density (e)Roughness (f)Engineering geological rock formations

(g)NDVI (h) SPI (i) Rainfall

Figure 2. Grading diagram of evaluation factors of ditch unit

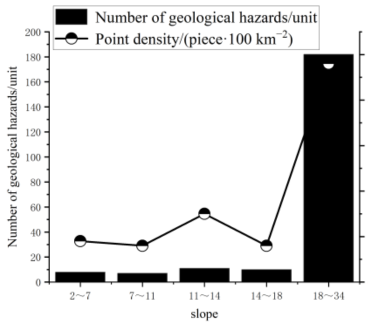

(a)Slope and geohazards

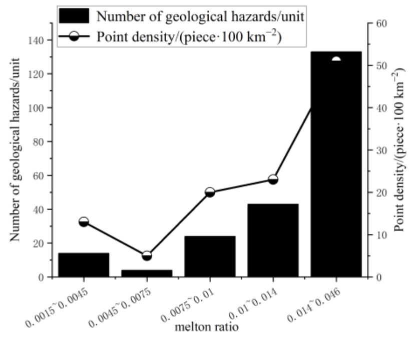

(b)Melton ratio and geohazards

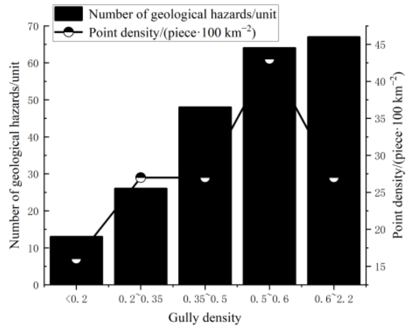

(c)Gully density and geohazards

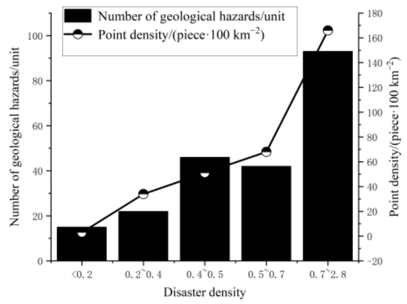

(d)Density disaster and geohazards

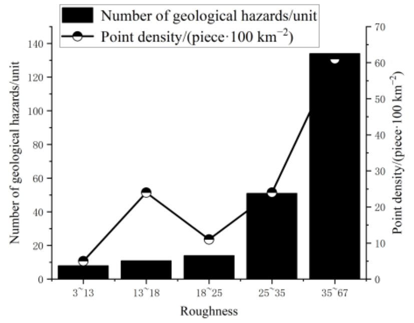

(e) Roughness and geohazards

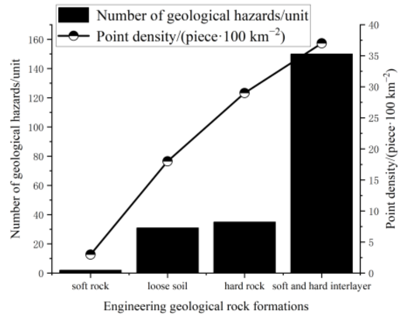

(f) Engineering geological rock formations and geohazards

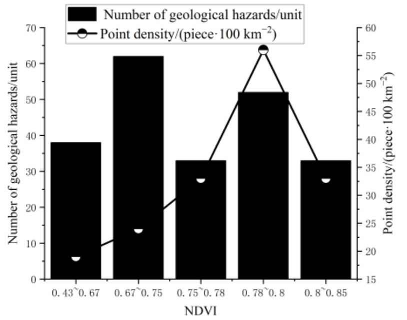

(g) NDVI and geohazards

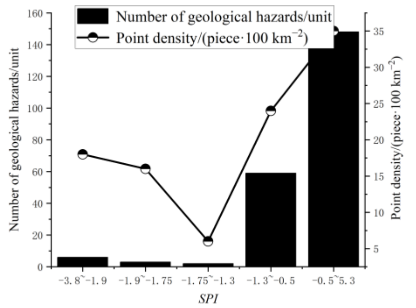

(h) SPI and geohazards

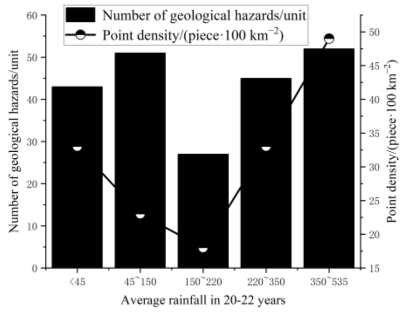

(i) Rainfall and geohazards

Figure 3. Statistical chart of the relationship between evaluation factors and geological hazards

6. Assessment of susceptibility to geological disasters

6.1. Weight of evaluation indicators

This study employs the Analytical Hierarchy Process (AHP) to systematically assign weights to indicators for evaluating geological hazards. Data normalization ensures consistency and comparability. SPSS software facilitates the necessary computations. Expert assessments construct the judgment matrix, and the Saaty method converts eigenvectors into standardized weight values. The highest weight is attributed to disaster point density (0.2942), while the Melton ratio holds the lowest weight (0.0257), reflecting their respective influences on the evaluation of geological hazards.

Table.2. Evaluation index weights and weighted information values

First level evaluation factor	serial number	Secondary evaluation factors	information value	Weights	Weighted information value
Slope	1	2~7	-7167	0.0453	-324.6651
	2	7~11	-8644		-391.5732
	3	11~14	-2547		-115.3791
	4	14~18	-9108		-412.5924
	5	18~34	9008		408.0624
Melton ratio	1	0.0015~0.0045	-8110	0.0257	-208.427
	2	0.0045~0.0075	-16775		-431.1175
	3	0.0075~0.01	-3663		-94.1391
	4	0.01~0.014	-2485		-63.8645
	5	0.014~0.046	5683		146.0531
Ravine density	1	<0.2	-6195	0.1249	-773.7555
	2	0.2~0.35	-862		-107.6638
	3	0.35~0.5	-732		-91.4268
	4	0.5~0.6	3979		496.9771
	5	0.6~2.2	-562		-70.1938
Disaster density	1	<0.2	-22269	0.2942	-6551.53
	2	0.2~0.4	1576		463.6592
	3	0.4~0.5	5686		1672.8212
	4	0.5~0.7	8542		2513.0564
	5	0.7~2.8	17464		5137.9088
Roughness	1	3~13	-16646	0.0453	-754.0638
	2	13~18	-1798		-81.4494
	3	18~25	-9735		-440.9955
	4	25~35	-1925		-87.2025
	5	35~67	7440		337.032
Engineering geological rock formations	1	1	-22484	0.1190	-2675.596
	2	2	-4463		-531.097
	3	3	110		13.09
	4	4	2573		306.187
NDVI	1	0.43~0.67	-4037	0.0232	-93.6584
	2	0.67~0.75	-2047		-47.4904
	3	0.75~0.78	1377		31.9464
	4	0.78~0.8	6526		151.4032
	5	0.8~0.85	1219		28.2808
SPI	1	-3.8~-1.9	-4692	0.1133	-531.6036
	2	-1.9~-1.75	-6050		-685.465
	3	-1.75~-1.3	-16464		-1865.371
	4	-1.3~-0.5	-1840		-208.472
	5	-0.5~5.3	1963		222.4079
Rainfall	1	<45	1323	0.2091	276.6393
	2	45~150	-2477		-517.9407
	3	150~220	-4985		-1042.36
	4	220~350	1248		260.9568
	5	350~535	5222		1091.9202

6.2. Evaluation index information amount

In order to more comprehensively incorporate the contributions of various evaluation indicators to geological disasters, the research utilizes a combined approach involving the information quantity model and the analytic hierarchy process. To achieve this objective, the weighted information volume calculation formula is employed, as expressed by Formula (7).

$$I=\sum_{i=1}^{n}(W_i \times I_i) \tag{7}$$

In the Formula (7): W_i ——The weight of the evaluation factor determined by the analytic hierarchy process. I_i ——The information content of the secondary evaluation factors determined by the information content model. *n*—the number of evaluation factors.

The calculation results of the weighted information value are detailed in Table 2.

6.3. Geological disaster susceptibility evaluation results

Employing ArcGIS software, this study overlays the information values derived from the nine evaluation indicators to assess their cumulative impact [11]. A higher composite information value indicates an increased risk of geological disasters within the evaluated ditch units. For 191 areas, the aggregated information values range from -13,792.5~8,007.3. Using the natural breakpoint method, the susceptibility levels are classified into four categories: extremely high susceptibility (3,000~8,007.3), high susceptibility (-4,000~3,000), medium susceptibility (-7,500.4~-4,000), and low susceptibility (-13,792.5~-7,500.4). This detailed analysis culminates in the creation of a geological disaster susceptibility map for Huixian City (Figure 4).

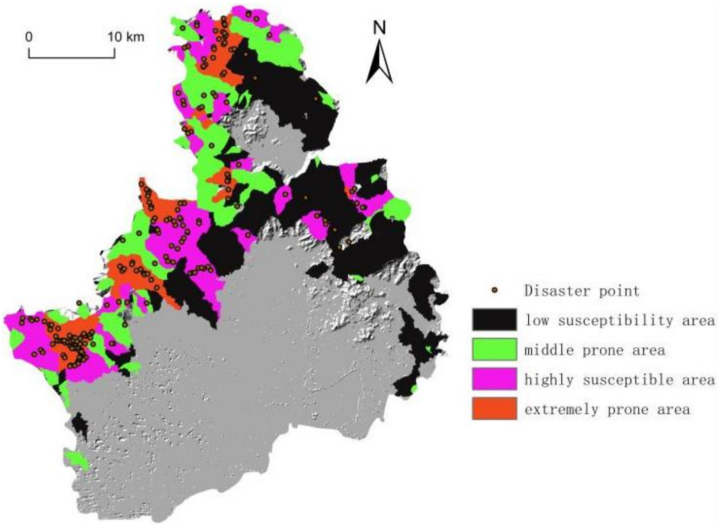

Figure 4. Geological disaster susceptibility assessment map of Huixian City

The map analysis, particularly in conjunction with Figure 4, shows that areas of extremely high and high susceptibility are mainly situated in the western parts of Huixian City, adjacent to the imposing Taihang Mountains. Characterized by steep terrain, widespread fault lines, fragmented bedrock and soil layers, and an accumulation of loose solids, these regions are also zones of intense human engineering activity. Construction efforts have extensively altered the natural landscape, exacerbating vulnerability. Consequently, these areas are prone to frequent, large-scale geological disasters, often triggered by variable rainfall patterns.

7. Evaluation results inspection and analysis

The study employed frequency ratio model and receiver operating characteristic curve (ROC) to assess the efficacy of the geological hazard evaluation model developed within this research.

(1) The geological hazard frequency ratio is used to measure the alignment between the susceptibility zoning levels and the actual distribution of disaster points. Ideally, areas identified with extremely high and high susceptibility would show a higher frequency ratio, while those deemed to have low susceptibility would have a lower ratio, indicating a closer match between evaluation results and real-world conditions. As illustrated in Table 3, the frequency ratio for areas in Huixian City with a high propensity for geological disasters peaks at 4.27, a stark contrast to the 0.014 ratio for areas with low susceptibility. Moreover, the frequency ratio increases alongside the susceptibility level, affirming the effectiveness of the proposed evaluation model in mirroring the actual distribution of geological hazards accurately and reasonably.

Table.3. Statistical table of geological disaster susceptibility evaluation results

susceptibility level	Area	Area percentage (%)	Number of disaster points/piece	Geological disaster percentage %	Frequency ratio
extremely prone area	96.31	12.77	119	54.6	4.27
highly susceptible area	176.18	23.36	84	38.5	1.65
middle prone area	171.14	22.69	12	5.5	0.24
low susceptibility area	310.59	41.18	3	1.4	0.014

(2) The Receiver Operating Characteristic (ROC) [12] curve is a critical tool for assessing model performance by segregating data thresholds and examining the precision of the outcomes. The Area Under Curve (AUC) [13] value, a standard measure for evaluating model efficacy in geological disaster susceptibility modeling, reflects the model's classification accuracy. An AUC value nearing 1 indicates a highly accurate model.

According to the data presented in Figure 5, the AUC value of the geological disaster susceptibility evaluation model for Huixian City is 0.871. This value, significantly higher than the 0.5 benchmark for random classification [14], highlights the model's substantial capacity to predict geological disasters accurately. With its high accuracy and dependability, the evaluation model proves to be an essential tool for categorizing disaster risk levels, offering a vital reference for implementing effective disaster prevention and control strategies.

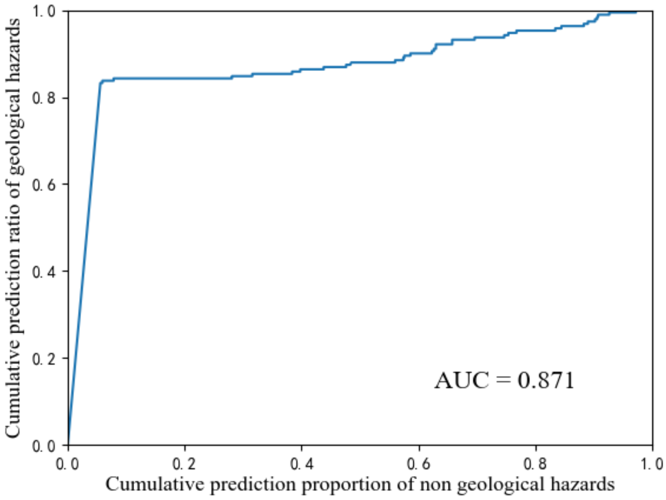

Figure 5. ROC curve of geological hazard susceptibility evaluation model

8. Conclusion

(1) Focusing on the ditch unit level, this research adopts an innovative method by combining the information volume model with the analytic hierarchy process for evaluating the susceptibility to geological disasters in Huixian City, southeast China. This integrated approach offers a precise depiction of the geomorphic features characteristic of geological disasters, thereby improving the utility and applicability of the evaluation outcomes.

(2) Through the application of ArcGIS and SPSS software, this study conducts a thorough assessment of geological disaster susceptibility in Huixian City using nine evaluation indicators. The analysis indicates that areas with extremely high and high susceptibility account for 36.13% of the total study area, underscoring the prevalent risk of geological disasters. In contrast, areas categorized as having low susceptibility feature fewer instances of geological disasters, aligning with the observed distribution patterns of these events.

(3) The robustness of the evaluation model's findings was substantiated using the frequency ratio model [15] and the Receiver Operating Characteristic (ROC) curve analysis. The frequency ratio escalates in tandem with rising levels of risk, with the ratio for areas at extreme risk significantly surpassing those at minimal risk. Furthermore, the evaluation model achieves an AUC value of 0.871, indicating its high precision and dependability. This underscores its substantial value in contributing to the monitoring and early warning systems for geological disasters.

Acknowledgements

I am profoundly grateful to Dr. Chen for their invaluable mentorship and consistent support during the manuscript's development. Your diligent review of my work and insightful feedback has been crucial in refining my paper. Your guidance has significantly enhanced my writing skills.

References

[1] Lin Degen, Hu Chuanqi, Lian Fang, et al. Risk Assessment of World Corn Salinization Hazard Factors Based on EPIC Model and Information Diffusion[J]. Land, 2023, 12(11): 2076.

[2] Puente-Sotomayor Fernando, Mustafa Ahmed, Teller Jacques. Landslide Susceptibility Mapping of Urban Areas: Logistic Regression and Sensitivity Analysis applied to Quito, Ecuador[J]. Geoenvironmental Disasters, 2021, 8(1): 19.

[3] Enjavinejad S. M., Zahedifar M., Moosavi A. A., et al. Integrated application of multiple indicators and geographic information system-based approaches for comprehensive assessment of environmental impacts of toxic metals-contaminated agricultural soils and vegetables[J]. Sci Total Environ, 2024, 926: 171747.

[4] Zhang S. H., Tan S. C., Liu L. F., et al. Slope Rock and Soil Mass Movement Geological Hazards Susceptibility Evaluation Using Information Quantity, Deterministic Coefficient, and Logistic Regression Models and Their Comparison at Xuanwei, China[J]. Sustainability, 2023, 15(13): 10466.

[5] Cao Juan, Zhang Zhao, Du Jie, et al. multi-geohazards susceptibility mapping based on machine learning—a case study in Jiuzhaigou, China[J]. Natural Hazards, 2020, 102(3): 851-871.

[6] Panchal S., Shrivastava A. K. Landslide hazard assessment using analytic hierarchy process (AHP): A case study of National Highway 5 in India[J]. Ain Shams Engineering Journal, 2022, 13(3): 101626.

[7] Qin X. L., Wang S. F., Meng M. Flood cascading on critical infrastructure with climate change: A spatial analysis of the extreme weather event in Xinxiang, China[J]. Advances in Climate Change Research, 2023, 14(3): 458-468.

[8] Marinos Vassilis, Carter Trevor G. Maintaining geological reality in application of GSI for design of engineering structures in rock[J]. Engineering Geology, 2018, 239: 282-297.

[9] Chen J., Xiao H. B., Li Z. W., et al. Threshold effects of vegetation coverage on soil erosion control in small watersheds of the red soil hilly region in China[J]. Ecological Engineering, 2019, 132: 109-114.

[10] Wang Jiaxi, Zhang Yan, Chen Chang, et al. Spatial variation in gully expansion rate in a loess-covered tableland region based on systematic sampling and high-resolution image interpretation[J]. Catena, 2024, 236: 107756.

[11] Li Yongchao, Chen Jianping, Tan Chun, et al. Application of the borderline-SMOTE method in susceptibility assessments of debris flows in Pinggu District, Beijing, China[J]. Natural Hazards, 2020, 105(3): 2499-2522.

[12] Sun Jianfeng, Yan Tiesheng, Hu Jinshu, et al. Slope-scale landslide susceptibility assessment based on coupled models of frequency ratio and multiple regression analysis with limited historical hazards data[J]. Natural Hazards, 2023, 120(1): 1-23.

[13] Juola J. F., Caballero-Sanz A., Munoz-Garcia A. R., et al. Familiarity, recollection, and receiver-operating characteristic (ROC) curves in recognition memory[J]. Mem Cognit, 2019, 47(4): 855-876.

[14] Martinez-Camblor P., Perez-Fernandez S., Diaz-Coto S. The area under the generalized receiver-operating characteristic curve[J]. Int J Biostat, 2021, 18(1): 293-306.

[15] Akinci H., Ozalp A. Y. Landslide susceptibility mapping and hazard assessment in Artvin (Turkey) using frequency ratio and modified information value model[J]. Acta Geophysica, 2021, 69(3): 725-745.